



Performance of Cu₂O/ZnO solar cell prepared by two-step electrodeposition

J. KATAYAMA, K. ITO, M. MATSUOKA* and J. TAMAKI

Department of Applied Chemistry, Faculty of Science and Engineering, Ritsumeikan University Nojihigashi, Kusatsu, Shiga 525-8577, Japan

(*author for correspondence, e-mail: matsuoaka@se.ritumei.ac.jp)

Received 5 September 2003; accepted in revised form 28 January 2004

Key words: cuprous oxide, electrodeposition, heterojunction solar cell, NESA substrate, zinc oxide

Abstract

Cu₂O/ZnO solar cells with improved performance were fabricated by an inexpensive two-step process. The process involves potentiostatic deposition of ZnO on NESA glass (tin-oxide-coated glass) followed by galvanostatic deposition of Cu₂O to form Cu₂O/ZnO/NESA solar cells with a short-circuit photocurrent density of 2.08 mA cm⁻², an open-circuit voltage of 0.19 V, a fill factor of 0.295 and conversion efficiency of 0.117%. The performance of the solar cells thus prepared is discussed in terms of the laminated structure, construction of the heterojunction, and the crystallinity and optical properties of each semiconductor.

1. Introduction

Cu₂O is a p-type semiconductor with a bandgap energy in the range of 1.96 eV to 2.38 eV, and has the potential to form a solar cell with high open-circuit voltage by combination with a suitable n-type semiconductor. Furthermore, Cu₂O has low toxicity and good environmental acceptability, is cheap and plentiful, and can be readily prepared as large-area samples. Schottky-barrier solar cells such as Cu₂O/Cu have been examined extensively, and have been prepared by thermal oxidation of a copper sheet [1] or anodic oxidation in alkaline solution [2]. Olsen et al. [3] pointed out that the relatively low conversion efficiency of Cu₂O/Cu solar cells is due to high barrier heights (0.7–0.9 eV), and suggested that the heterojunction or metal insulator semiconductor device structure could be modified to improve efficiency.

Extensive research concerning heterojunction solar cells based on Cu₂O has been carried out by Trivich [4] and Scharl [5], and their results were reviewed by Rai [6]. They found that metallic copper or copper-rich regions occurred at the ZnO/Cu₂O interface as a result of thermal reaction. However, neither oxygen depletion nor copper enrichment were detected at the interface of CdO/Cu₂O heterojunctions prepared at room temperature [4, 6]. These heterojunctions were reported to have an open-circuit voltage (V_{oc}) of 0.4 V and short-circuit current density (J_{sc}) of 2 mA cm⁻², indicating that the formation of the heterojunction at low temperature is favourable for improving photovoltaic performance.

Electrodeposition, which can be performed at low temperature, is therefore the most suitable method for producing high-quality heterojunction solar cells, avoid-

ing the unfavourable reactions that occur at elevated temperatures. In this study, ZnO was selected as a candidate n-type semiconductor because of its stability in the presence of Cu₂O and its suitability as a window material (reported bandgap of 3.3–3.5 eV).

The manufacture of a thin semiconductor film by electrodeposition allows for precise control of film thickness and is relatively inexpensive. Lincot [7, 8] and Izaki [9–11] have reported the electrodeposition of ZnO from aqueous solution. In this study, the potentiostatic electrolysis from a zinc nitrate solution reported by Izaki was employed. While Switzer [12, 13] reported the electrodeposition of Cu₂O from an alkaline copper(II) lactate solution, lactic acid is corrosive and unstable in air. Therefore, Cu₂O films were electrodeposited in the present study from an alkaline copper(II) sulfate solution containing non-toxic DL-malic acid as a complexing agent.

Tak et al. [14] reported the selective electrodeposition of ZnO on Cu₂O, but the performance of the product as a solar cell material was not evaluated. In this study, a solar cell with the structure Cu₂O/ZnO/NESA was fabricated by two-step electrodeposition and its performance evaluated.

2. Experimental details

In a preliminary experiment, a satisfactory p–n junction could not be constructed by depositing ZnO onto Cu₂O due to partial reduction of Cu₂O to metallic copper during the electrodeposition of ZnO. As a result, the p–n junction was fabricated by the galvanostatic deposition of Cu₂O after potentiostatic deposition of the ZnO layer

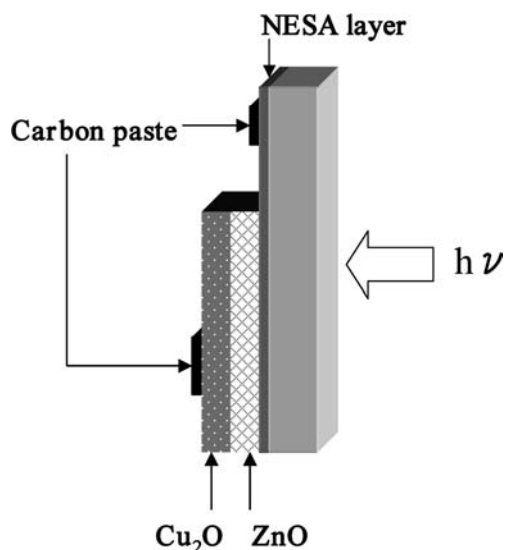


Fig. 1. Schematic representation of $\text{Cu}_2\text{O}/\text{ZnO}$ cell prepared by two-step electrodeposition.

on NESAs glass. A schematic representation of the heterojunction solar cell produced in this way is shown in Figure 1.

Cu_2O was electrodeposited from an aqueous electrolyte onto transparent conductive substrates (NESAs glass with a sheet resistance of $10 \Omega/\square$) or ZnO film on NESAs glass. The electrolyte consisted of $0.10 \text{ mol dm}^{-3} \text{ CuSO}_4$ and 0.25 mol dm^{-3} malic acid, adjusted to pH 9.0 with NaOH . The Cu_2O film was cathodically electrodeposited at constant current densities of -0.1 to -0.5 mA cm^{-2} using a potentiogalvanostat (HA-201, Hokuto Denko). Before each experimental run, the NESAs glass was ultrasonicated in acetone for 30 s and then anodically electrolysed in $1 \text{ mol dm}^{-3} \text{ NaOH}$ solution at a current density of 1 mA cm^{-2} for 60 s. Electrodeposition was then carried out at 333 K using a Pt plate as a counter electrode.

ZnO film was prepared by a potentiostatic technique in a three-electrode system using an Ag/AgCl electrode as the reference and Pt plates as counter electrodes. ZnO film was electrodeposited on NESAs substrates at -0.8 V vs Ag/AgCl from a $0.1 \text{ mol dm}^{-3} \text{ Zn}(\text{NO}_3)_2$ solution at 333 K. The film thickness was controlled by a coulometer (HF-201, Hokuto Denko) fitted to the potentiogalvanostat.

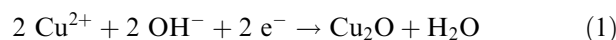
The deposited Cu_2O and ZnO films were characterized by X-ray diffraction (XRD; Rint-2000, Rigaku) for identification and determination of crystallographic parameters. The surface morphology of a single layer and a cross section of the laminated semiconductors was examined by scanning electron microscopy (SEM; JSM-6335F, Jeol). The optical absorption spectrum of Cu_2O and ZnO deposited on NESAs glass was measured at wavelengths from 200 to 700 nm using a spectrophotometer (UV-2500PC, Shimadzu). The conduction type of the film was identified from the photocurrent response indicated by the polarization curve for the Cu_2O and ZnO electrodes in $0.1 \text{ mol dm}^{-3} \text{ K}_2\text{SO}_4$

solution. A xenon short-arc lamp (SX-UID500XCM, Ushio) was used as the light source. Composition analysis was performed by X-ray photoelectron spectrometry (XPS; ESCA-5800, Ulvac-Phi) in the depth direction of the $\text{ZnO}/\text{Cu}_2\text{O}$ junction laminated on NESAs glass. An Ar ion gun with a sputtering speed of 4 nm min^{-1} for the SiO_2 reference was used for etching the sample. The effect of exposure to light on resistance was evaluated using a sample prepared by depositing a $1 \mu\text{m}$ thick Cu_2O layer on NESAs glass, then screen-printing carbon paste (Electrodag 581SS, Acheson) in a comb shape onto the sample, as reported elsewhere [11], and finally annealing at 427 K in air. The photoresponse of resistance was then measured using a digital multimeter (5430, Soar). A solar simulator (YSS-80, Yamashita Denso; AM 1.5, 120 mW) was used for measurement of photovoltaic properties.

3. Results and discussion

When cathodic current is applied to an electrode immersed in an alkaline copper(II) sulfate solution containing malic acid as a complexing agent, Cu^{2+} ions are reduced to Cu_2O or Cu depending on the current density, as indicated by the following equations [15]:

Low current density



High current density



Typical potential curves during electrodeposition at constant current densities of -0.3 and -0.5 mA cm^{-2} are shown in Figure 2. During galvanostatic deposition at -0.5 mA cm^{-2} , a periodic potential oscillation is observed, representing alternating Cu_2O and Cu deposition as reported by Switzer [12, 13] and Leopold [15].

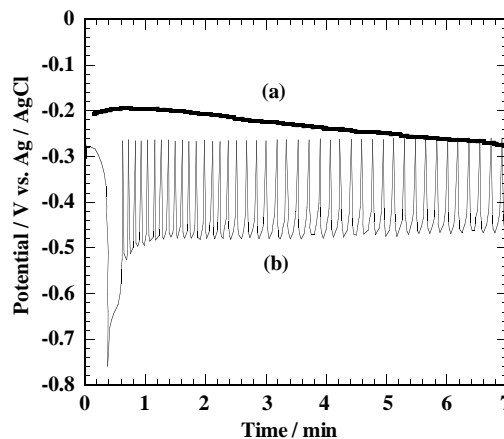


Fig. 2. Potential-time curve for NESAs electrode in a solution of $0.1 \text{ mol dm}^{-3} \text{ CuSO}_4$ and 0.25 mol dm^{-3} malic acid at pH 9.0. Current density: (a) -0.3 and (b) -0.5 mA cm^{-2} .

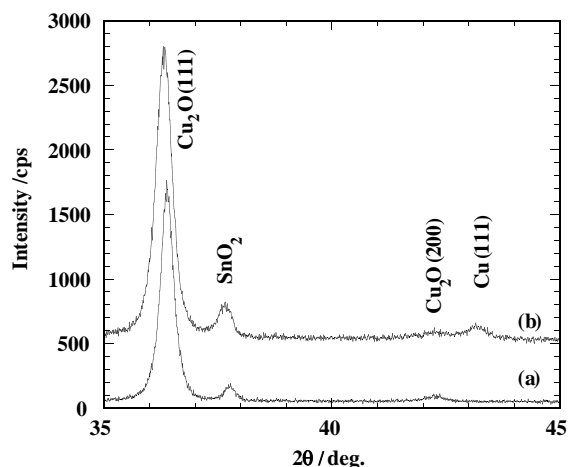


Fig. 3. XRD patterns of Cu_2O films prepared at different current densities from a solution of 0.10 mol dm^{-3} CuSO_4 and 0.25 mol dm^{-3} malic acid at pH 9.0. Current density: (a) -0.3 and (b) -0.5 mA cm^{-2} .

This potential oscillation is not apparent at -0.3 mA cm^{-2} . In this case, the deposition potential shifted from -0.2 to -0.3 V with increasing thickness of deposited Cu_2O due to its high resistance.

The XRD profiles of the films deposited on NESA glass at -0.3 and -0.5 mA cm^{-2} are shown in Figure 3. For the sample prepared at -0.3 mA cm^{-2} , all the diffraction peaks are attributed to Cu_2O except for a single SnO_2 line, indicating that the deposit is pure crystalline Cu_2O . The lattice parameter of the film was found to be $a = 0.4275 \text{ nm}$ (cf. JCPDS 5-667; $a = 0.4270 \text{ nm}$). The apparent crystallite size is 37 nm , as calculated using Scherrer's equation ($D = 0.94 \lambda / \beta_{1/2} \cos \theta$; where λ is the wavelength of CuK_α radiation and $\beta_{1/2}$ the half-width of the diffraction line). Pure crystalline Cu_2O was obtained at current densities of -0.1 to -0.4 mA cm^{-2} . A diffraction line attributable to $\text{Cu}(111)$ was detected at $2\theta = 43^\circ$ for the film deposited at -0.5 mA cm^{-2} . In this case, nano-sized Cu and crystalline Cu_2O are deposited alternately, induced by periodic fluctuation in pH at the electrode surface [13].

The surface morphologies of Cu_2O films deposited at constant current densities of -0.1 to -0.3 mA cm^{-2} are shown in Figure 4. In each case, the deposition time was controlled to ensure a current of 1 C cm^{-2} . The Cu_2O film deposited at -0.1 mA cm^{-2} was pyramidal in shape and relatively large, about $3 \mu\text{m}$. In this case, the substrate was partially exposed between pyramidal

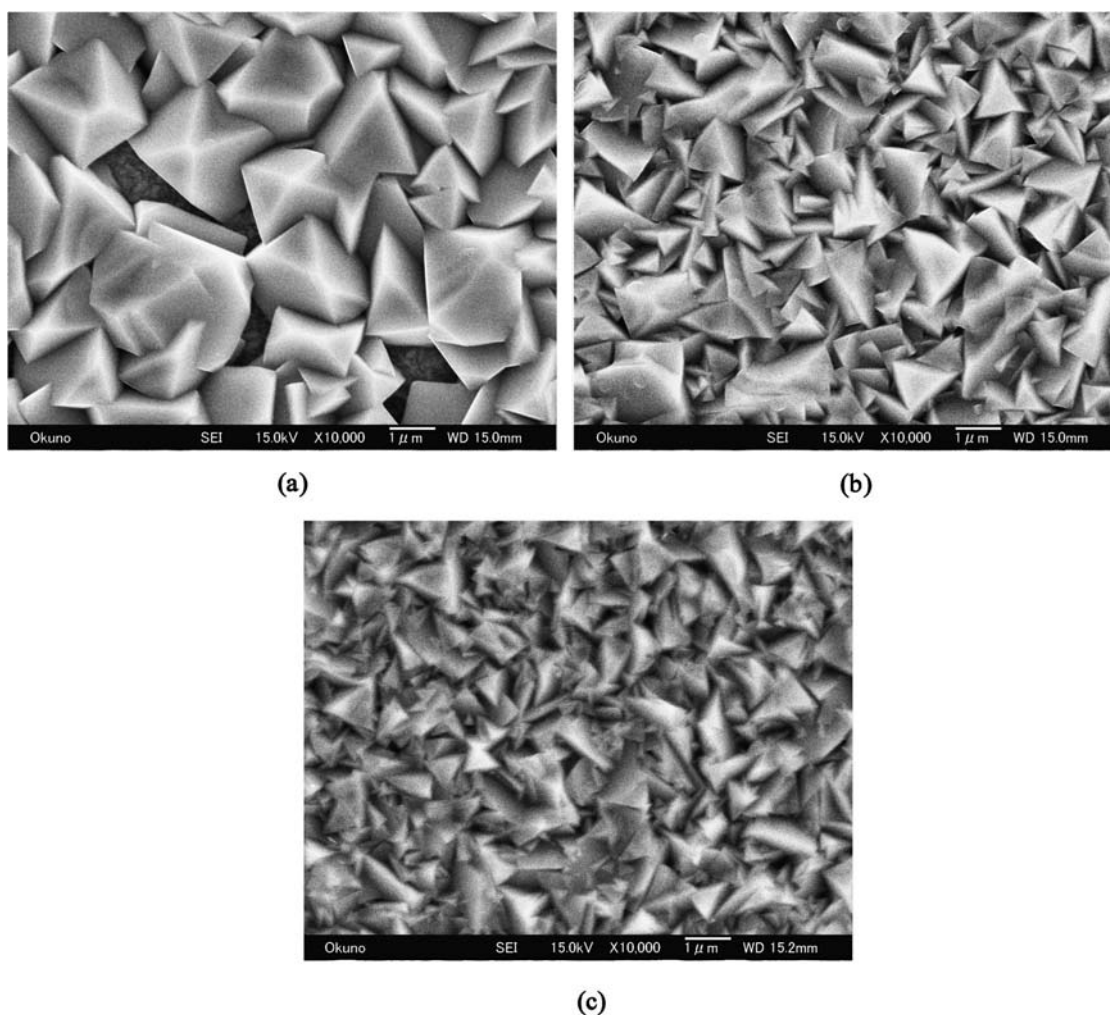


Fig. 4. SEM images of Cu_2O films deposited at various current densities: (a) -0.1 , (b) -0.2 and (c) -0.3 mA cm^{-2} .

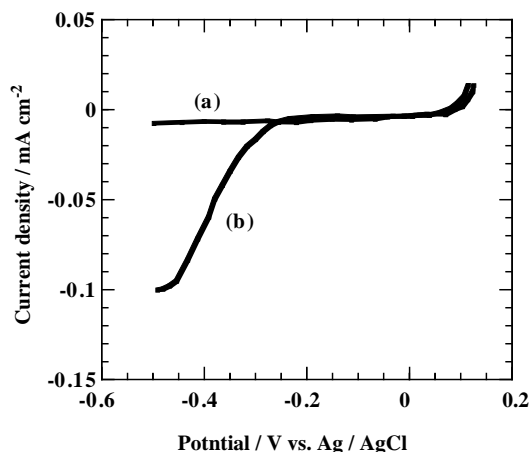


Fig. 5. Current-potential curve for a Cu_2O electrode in 0.1 mol dm^{-3} K_2SO_4 solution. (a) In the dark, (b) under photoirradiation.

Cu_2O particles. However, this exposure diminished as the crystals became finer at cathodic current densities exceeding -0.2 mA cm^{-2} .

To confirm the conduction type of the deposited film, the photoresponse of the polarization curve for the Cu_2O film prepared at -0.3 mA cm^{-2} was measured in 0.1 mol dm^{-3} K_2SO_4 solution. The results are shown in Figure 5. Cathodic current was not detected in the dark, but a distinct photocurrent was generated when exposed to light, indicating that the Cu_2O film is a p-type semiconductor. The optical properties of Cu_2O were also evaluated based on the absorption spectra of the film deposited on NESA glass. The bandgap energy obtained from the spectral data is $\sim 2.1 \text{ eV}$, which is in reasonable agreement with that reported for Cu_2O film deposited from alkaline copper(II) lactate solution [12]. The bandgap energy of Cu_2O film deposited galvanostatically at current densities of -0.1 to -0.4 mA cm^{-2} was relatively constant and independent of the applied current density.

The photoresponse of the resistance of Cu_2O film deposited on NESA glass was evaluated using the comb-shaped electrode printed onto the sample with carbon paste. The results for normalized resistance are shown in Figure 6. The normalized resistance is defined as $R = 100R_{\text{light}}/R_{\text{dark}}$, where R_{light} is the resistance under photoirradiation and R_{dark} ($1.53 \text{ k}\Omega$) is the resistance of the sample after 2 h in the dark. The resistance rapidly decreases upon photoirradiation, but increases only slowly when the light is interrupted. This slow response of resistance change upon light interruption is partly due to the heating effect, inhibiting the recombination of electrons and holes.

A $\text{Cu}_2\text{O}/\text{ZnO}$ solar cell was then prepared by a two-step electrochemical method. In the first step, ZnO film was deposited on NESA glass to construct the heterojunction. The ZnO film was deposited potentiostatically at -0.8 V vs Ag/AgCl from an aqueous solution containing 0.1 mol dm^{-3} $\text{Zn}(\text{NO}_3)_2$ by passing a current of 1 C cm^{-2} . The ZnO deposition reaction from deaerated zinc nitrate solution is described as follows [16]:

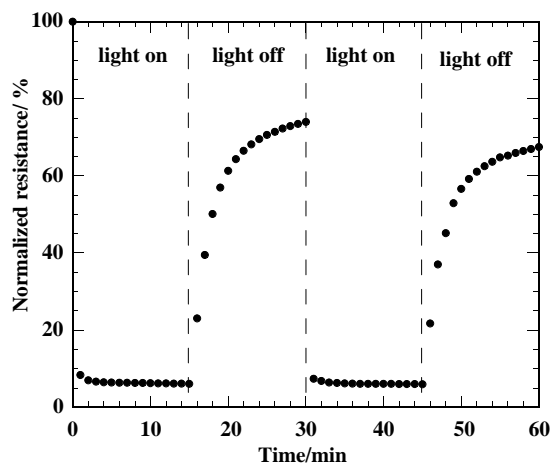
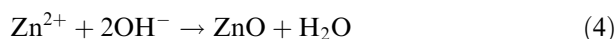
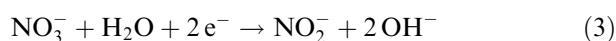


Fig. 6. Effect of photoirradiation on normalized resistance of Cu_2O films prepared at -0.3 mA cm^{-2} .



XRD analysis of the ZnO film revealed that the deposit has a hexagonal structure with lattice parameters of $a = 0.3259 \text{ nm}$ and $c = 0.5215 \text{ nm}$ (cf. JCPDS36-1451; $a = 0.3250 \text{ nm}$, $c = 0.5207 \text{ nm}$). Using Scherrer's equation, the apparent crystallite size of ZnO is 76 nm . The detected anodic photocurrent response of the ZnO electrode in 0.1 mol dm^{-3} K_2SO_4 solution indicates n-type conduction. The bandgap energy evaluated from the absorption spectrum is 3.3 eV , and the carrier concentration of the ZnO film deposited at -0.8 V is estimated to be $\sim 10^{18} \text{ cm}^{-3}$, consistent with previous reports [11].

In the second step, Cu_2O film was deposited onto the ZnO/NESA sample from an alkaline copper(II) malate solution at a constant current density of -0.3 mA cm^{-2} by passing a current of 1 C cm^{-2} . This process established the p-n junction. Ohmic contact was achieved using carbon paste, and the sample was finally annealed for 30 min at 423 K in air.

A cross-sectional SEM micrograph of the $\text{Cu}_2\text{O}/\text{ZnO}/\text{NESA}$ solar cell is shown in Figure 7. The ZnO and Cu_2O films are each about $1 \mu\text{m}$ thick, in reasonable agreement with the thickness calculated from the current passed in deposition. The films form a layered structure, yielding a good heterojunction.

The results of compositional analysis in the depth direction at the heterojunction are shown in Figure 8. Scharl et al. reported an oxygen deficiency at the heterojunction of ZnO/ Cu_2O structures prepared by RF sputtering of ZnO on Cu_2O due to the reduction of Cu_2O by residual hydrogen in the chamber [5]. However, no such unfavourable phenomenon was detected, with Cu_2O and ZnO present in stoichiometric proportions and the successful formation of a satisfactory heterojunction. The rectification property of the

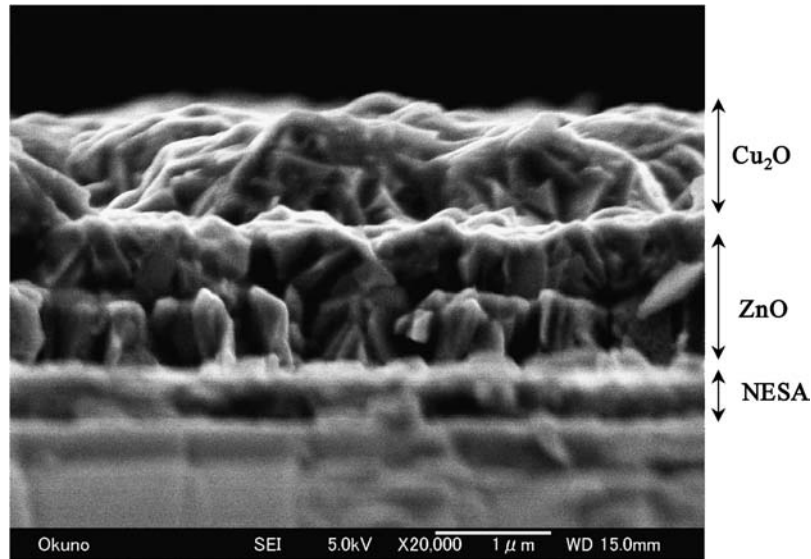


Fig. 7. SEM image of cross-section of electrochemically prepared $\text{Cu}_2\text{O}/\text{ZnO}$.

$\text{Cu}_2\text{O}/\text{ZnO}$ heterojunction was evaluated by applying a bias of +0.8 V and -0.8 V to the sample. The current in the forward direction was 0.92 mA, and that in the reverse direction was 0.13 mA, giving a rectification ratio of ~ 7 .

The photocurrent response to irradiation with a xenon short-arc lamp is shown in Figure 9. The photocurrent immediately builds up to $110 \mu\text{A}$ upon photoirradiation, and only drops gradually to zero when the light is interrupted. However, the current decay rate is considerably rapid compared to the recovery rate of resistance as shown in Figure 6.

The photovoltaic properties of the $\text{Cu}_2\text{O}/\text{ZnO}$ solar cell were evaluated using a solar simulator (incident light AM 1.5, 120 mW cm^{-2}). The results are shown in Figure 10. The short-circuit photocurrent density, open-

circuit voltage, fill factor, and conversion efficiency were found to be 2.08 mA cm^{-2} , 0.19 V, 0.295 and 0.117%, respectively. This characteristic is superior to that ($J_{\text{sc}} = 1.4 \text{ mA cm}^{-2}$, $V_{\text{oc}} = 0.18 \text{ V}$) of a solar cell prepared at 423 K by sputtering In-doped ZnO on Cu_2O [5]. However, the conversion efficiency is insufficient for practical use. It is considered that defects induced by mismatch between the lattice parameters at the heterojunction may be responsible for the low efficiency, as well as light reflection from the surface of the NESA glass and low transmittance of ZnO at the wavelengths of light in the present experiments (transmittance at $600 \text{ nm} = 45\%$). Further improvement of the conversion efficiency is therefore expected to be possible by eliminating lattice-mismatch defects, which act as recombination centers, and by increasing the transmittivity of ZnO film and reducing the resistance of Cu_2O .

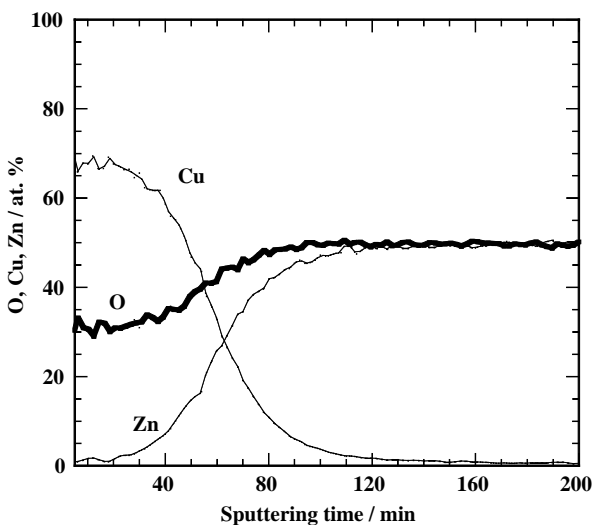


Fig. 8. Concentration profiles for O, Cu and Zn as a function of sputtering time in $\text{Cu}_2\text{O}/\text{ZnO}$ laminate.

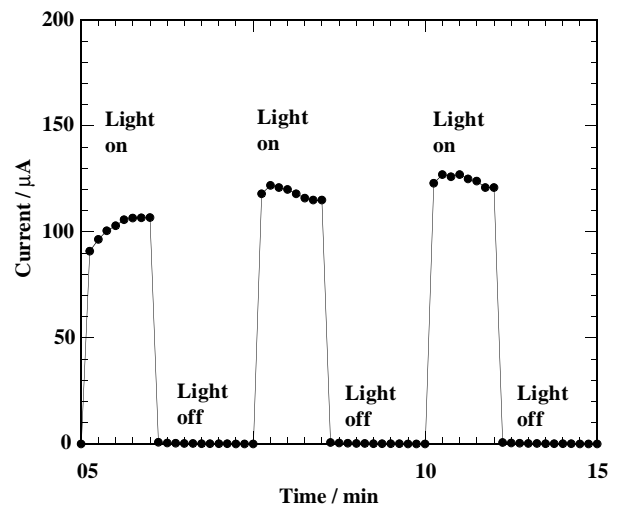


Fig. 9. Effect of photoirradiation on current generation in $\text{Cu}_2\text{O}/\text{ZnO}$ cell.

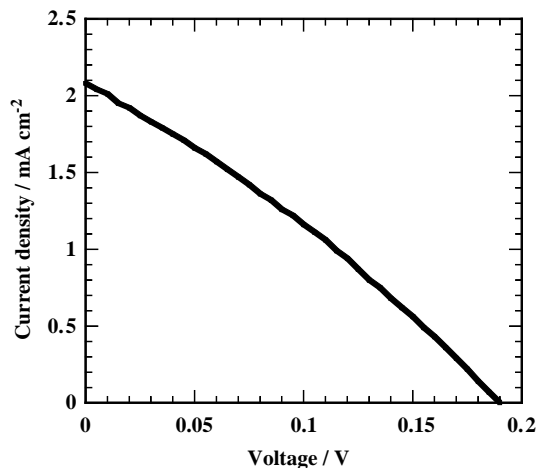


Fig. 10. Photovoltaic output of $\text{Cu}_2\text{O}/\text{ZnO}$ cell under AM 1.5 condition.

4. Conclusions

Pure crystalline Cu_2O was deposited at current densities of -0.1 to -0.4 mA cm^{-2} from alkaline copper(II) sulfate solution containing malic acid as a complexing agent (pH 9.0). The Cu_2O film deposited at -0.3 mA cm^{-2} was composed of fine crystals, and p-type conduction was confirmed by photoelectrochemical measurement. The bandgap energy of the Cu_2O was found to be 2.1 eV. The ZnO film provided n-type conduction and had a bandgap energy of 3.3 eV.

A p- $\text{Cu}_2\text{O}/\text{n-ZnO}/\text{NESA}$ solar cell produced by two-step electrodeposition was shown to have an excellent p-n junction, as confirmed by cross-sectional SEM analysis and XPS compositional analysis. Distinct rectification and photocurrent responses were detected for the solar cell. Under conditions of AM 1.5, the solar cell

exhibited a short-circuit current density of 2.08 mA cm^{-2} , an open-circuit voltage of 0.19 V, a fill factor of 0.295, and a conversion efficiency of 0.117%.

Acknowledgements

The authors thank Prof. Takakura of the Department of Photonics, Ritsumeikan University and all staff in his laboratory for helpful discussions and assistance in the assembly and operation of the solar simulator.

References

1. G.A. Adegboyega, *Solar & Wind Technol.* **2** (1985) 191.
2. E. Fortin and D. Masson, *Solid-State Electron.* **25** (1982) 281.
3. L.C. Olsen, R.C. Bohara and M.W. Urie, *Appl. Phys. Lett.* **34** (1979) 47.
4. L. Papadimitriou, N.A. Economou and D. Trivich, *Solar Cells* **3** (1981) 73.
5. J. Herion, E.A. Niekisch and G. Scharl, *Sol. Energy Mater.* **4** (1980) 101.
6. B.P. Rai, *Solar Cells* **25** (1988) 265.
7. S. Peulon and D. Lincot, *Adv. Mater.* **8** (1996) 166.
8. S. Peulon and D. Lincot, *J. Electrochem. Soc.* **145** (1998) 864.
9. M. Izaki and T. Omi, *Appl. Phys. Lett.* **68** (1996) 2439.
10. M. Izaki and T. Omi, *J. Electrochem. Soc.* **143** (1996) L53.
11. J. Katayama and M. Izaki, *J. Appl. Electrochem.* **30** (2000) 855.
12. T.D. Golden, M.G. Shumsky, Y. Zhou, R.A.V. Werf, R.A.V. Leeuwen and J.A. Switzer, *Chem. Mater.* **8** (1996) 2499.
13. J.A. Switzer, C-J. Hung, L-Y. Huang, F.S. Miller, Y. Zhou, E.R. Taub, M.G. Shumsky and E.W. Bohannan, *J. Mater. Res.* **13** (1998) 909.
14. J. Lee and Y. Tak, *Electrochem. Commun.* **2** (2000) 765.
15. S. Leopold, M. Herranen and J.O. Carisson, *J. Electrochem. Soc.* **148** (2001) C513.
16. J. Lee and Y. Tak, *J. Ind. Eng. Chem.* **5** (1999) 87.